Charge-Transfer Excited States of Ruthenium(II) Complexes. I. Quantum Yield and Decay Measurements[1,2]

G. D. Hager[3] and G. A. Crosby*

Contribution from the Department of Chemistry, Washington State University, Pullman, Washington 99163. *Received November 19, 1974*

Abstract: Quantitative measurements of the luminescence spectra, decay times, and quantum yields of ruthenium(II) cations of D_3 symmetry containing 2,2′-bipyridine and substituted-bipyridine ligands have yielded energy-level splittings and radiative and radiationless decay constants for the states arising from the $d\pi^*(a_2)$ charge-transfer configuration. The derived radiative rate constants provide additional evidence for the state symmetry assignments previously proposed. Rapid thermal relaxation among emitting levels is observed and attributed to strong spin-orbit coupling tying the spins to the lattice. The polarization characteristics of the emitted radiation is predicted to be strongly temperature dependent. Detailed descriptions of the techniques for making the measurements are included. Extension of both the techniques and interpretations to other ions displaying charge-transfer luminescence is discussed.

Recently a group theoretic coupling model was proposed to rationalize the measured decay times of the photoluminescences observed from the tris(2,2′-bipyridine)ruthenium(II) and tris(4,4′-diphenyl-2,2′-bipyridine)ruthenium(II) cations and *cis*-dicyanobis(2,2′-bipyridine)ruthenium(II).[4] The model was devised to account for the dependences of the decay times of these systems on temperature and magnetic field strength and to allow provisional symmetry labels to be assigned to the manifold of excited levels responsible for the intense orange photoluminescence emanating from complex ions of this type. The present series of investigations was undertaken to test further the validity of the proposed coupling model for charge-transfer (CT) excited states and to provide a quantitative measurement of the fundamental molecular parameters controlling their optical properties. In particular we set out to answer the following questions. (a) Do the state symmetry assignments proposed on the basis of a comparison of selection rules with *measured* decay rates of excited states hold up when tested against the *radiative* decay rates of the levels? (b) Can the energy-level splittings derived from computer analyses of decay time curves be observed directly by monitoring spectral changes with temperature? (c) Can quantitative information on the radiationless rate constants for the individual sublevels be obtained and correlated with structure? (d) What is the relationship of the experimentally determined rate constants and splittings of the observed excited states to the ligand π electronic structure? Can delocalization of the promoted electron over the π system be measured and correlated with the detailed structures of the surrounding ligands? What is the origin and magnitude of ligand–ligand interaction in complexes of this type? (e) What is the role of the central metal ion, in particular its strong spin-orbit forces, in governing the disposition and natures of the CT excited states? (f) Are there fundamental molecular parameters that can be extracted from measurements on CT excited states of one molecule and be transferred with confidence to other similar molecular systems? (g) Is the proposed coupling model extensible to the charge-transfer-to-ligand excited states of complexes with other metals, other ligands, and other symmetries? (h) How far can the proposed model be quantified and still retain relative simplicity? What further experimental checks can be made on its validity? What are its predictive capabilities? Where does it fail? (i) What is the relationship of the spectroscopically defined CT excited states to the photochemical properties of these materials and, ultimately, to their electrochemical and chemical behaviors?

In this article attention is focused on quantitative spectroscopic investigations of ruthenium(II) cations of D_3 symmetry containing 2,2′-bipyridine and substituted bipyridine ligands. In the succeeding one analogous results on a set of ruthenium(II) species containing *o*-phenanthroline and substituted *o*-phenanthroline ligands are analyzed, compared to those of the bipyridine series, and correlated with structure.[5] In the third article a detailed mathematical development of the proposed coupling model is presented, and quantitative assessments of the role of excited state charge distribution and spin-orbit coupling in determining CT level splittings in molecules of this type are made.[6]

Experimental Section

Preparation and Purification of Samples. Tris(2,2′-bipyridine)ruthenium(II) chloride hexahydrate, $[Ru(bpy)_3]Cl_2$, was purchased from G. Frederick Smith Company and was used without further purification. The sample of tris(4,4′-diphenyl-2,2′-bipyridine)ruthenium(II) chloride, $[Ru(4,4'\text{-}Ph_2bpy)_3]Cl_2$, was synthesized and analyzed previously,[7] and the tris(4,4′-dimethyl-2,2′-bipyridine)ruthenium(II) chloride tetrahydrate, $[Ru(4,4'\text{-}Me_2bpy)_3]Cl_2$, was prepared and purified by the methods employed in this laboratory for analogous complexes.[7]

Anal. Calcd for $[Ru(C_{12}H_{12}N_2)_3]Cl_2 \cdot 4H_2O$: C, 54.82; H, 5.58; Cl, 9.01; N, 10.65. Found: C, 54.61; H, 5.44; Cl, 8.35; N, 10.66.

Preparation of Plastics. To facilitate sample handling over large temperature ranges, the three complexes were studied in polymethylmethacrylate (PMM) matrices. The rigid doped plastic matrices were prepared by dissolution of both the complex and PMM in chloroform and then removal of the solvent under vacuum. The resultant solid solutions had a uniform color and showed no sign of solute crystallization. The PMM displayed no significant absorption in the visible and near-uv regions down to 370 nm, and repeated exposures of the samples to thermal stresses and to high intensity uv and visible radiation produced no measurable deterioration.

Spectra. Photoluminescence spectra both at 77 and 4.2 K were recorded with a red-sensitive spectrometer constructed in this laboratory.[8] Excitation was achieved by passing light from a 1000-W Hg–Xe lamp through 5 cm of aqueous $CuSO_4$ (100 g/l.) and a Corning 7-60 uv filter. For recording the 77 K spectra the plastics were suspended in liquid nitrogen in a quartz dewar. The 4.2 K spectra were measured on the same samples immersed in liquid helium in an Andonian Model 0-24/7M-H dewar. The luminescence spectrum of $[Ru(4,4'\text{-}Me_2bpy)_3]Cl_2$ was also measured in a rigid ethanol–methanol (4:1, v/v) glass at 77 K. Excitation conditions were the same as those for stimulating the plastic samples. The absorption spectrum of this latter molecule was recorded at room temperature and at 77 K in the ethanol–methanol solvent with a Cary Model 14 spectrometer. Both the absorption and the luminescence (77 K) of each of the other two molecules dissolved in this same solvent system have been reported previously.[7,9]

Quantum Yields. The absolute quantum yields of $[Ru(bpy)_3]Cl_2$[10] and $[Ru(4,4'\text{-}Ph_2bpy)_3]Cl_2$[11] at 77 K in ethanol–

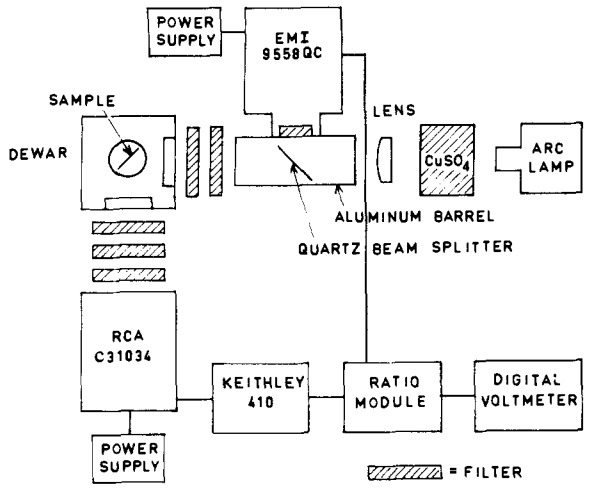

Figure 1. Block diagram of apparatus for relative intensity measurements.

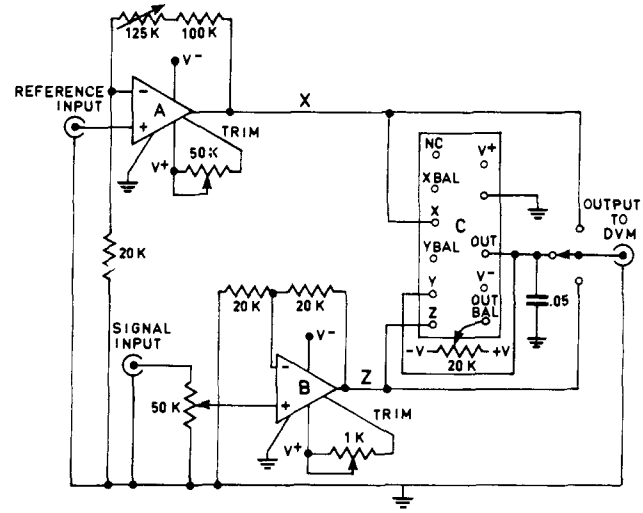

Figure 2. Schematic wiring diagram of the ratio recording dividing module: (amplifiers) A, Analog Devices 118K; B, Analog Devices 40J; (multiplier divider) C, Analog Devices 426A.

methanol glasses have been reported previously. The yield of $[Ru(4,4'-Me_2bpy)_3]Cl_2$ in a rigid ethanol–methanol glass at 77 K was measured[12] by the modified Parker-Rees technique used in this laboratory that has been described in detail elsewhere.[10,11] The standard, the excitation and filter systems, and the experimental techniques for obtaining spectra and absorbances were identical with those presented previously. No photochemical decomposition of the sample in the light beam was apparent.

Decay Time Measurements. The lifetime of the luminescence from each complex in the PMM matrix was measured in the same Andonian dewar used for obtaining the spectra. The operation and the temperature control of this particular system have been described previously.[4,13] One-centimeter squares of the doped plastics were subjected to the intense filtered uv light from an EG&G FX-12 flashlamp. The filtered light output was monitored by an EMI 9558QC photomultiplier and displayed on a Tektronix 535A oscilloscope. Mean decay times, recorded for all three complexes between ~1.8 and 77 K, were determined by a linear least-squares fit of ln intensity vs. time. Even at the lowest temperatures reached no deviations from exponential behavior were detected. The decays could be followed for several mean lives at the low temperatures.

Relative Intensity Measurements. To obtain a measurement of luminescence intensity as a function of temperature a ratio recording apparatus was designed and constructed. Two sets of data were recorded under different experimental conditions; only the experimental setup for the preferred set of measurements is described here in detail (Figure 1). Light from the 1000-W Hg–Xe arc lamp was first passed through 5 cm of aqueous $CuSO_4$ solution (200 g/l.). This solution transmitted from 330 to 580 nm and served to define partially the excitation band and to block the intense ir radiation emanating from the arc. The light was then focused to fill the full 1-in. aperture of the aluminum barrel containing a quartz beam splitter. Light deflected by the beam splitter passed through a neutral density filter and fell onto the photocathode of an EMI 9558QC photomultiplier that generated a reference signal for the ratio module. The main light beam passed through an Optics Technology 450 redpass and a Corning 7-59 glass filter before falling on the sample mounted in the dewar, which was equipped with fused quartz windows. Together with the $CuSO_4$ solution these two filters defined a broad excitation band spanning 430–480 nm.

Emitted light passed through a pair of Corning 3-69 glass filters and a neutral density filter (OD = 2.0) onto the photocathode of a RCA C31034 photomultiplier. The transmission characteristics of this particular filter system were checked and found to be virtually flat between 540 and 800 nm, the wavelength region of the monitored emissions. The RCA C31034 tube possesses a nearly flat quantum efficiency in the region between 500 and 800 nm, a necessary requirement for using it as a quantum counter.[14] Photocurrents in the range of 1.0 μA generated by this detector were fed into a Keithley Model 410 microammeter, which, in this apparatus, functioned as a current to voltage converter and amplifier. The temperature dependent output voltage from the Keithley was then applied to the ratio module.

Shown in Figure 2 is a schematic wiring diagram of the ratio module. The reference and signal voltages were adjusted to appropriate levels by the variable gain amplifiers A and B before being applied to the multiplier divider C. In the dividing configuration the output is $10Z/X$ where Z is the amplified signal voltage and X is the amplified reference voltage. By means of this experimental arrangement raw voltage data, proportional to the integrated intensities, were recorded for each of the complexes between ~4.5 and 77 K. Changes in the intensity of emitted light due to fluctuations of the exciting source were reduced to negligible values. The relative intensity curves recorded for the samples in PMM were normalized at 77 K to the known quantum yields obtained from ethanol–methanol glasses at this temperature.

As mentioned above the temperature dependent relative quantum yields were also measured with an experimental arrangement differing from that described. To indicate the reliability of our procedures and to give an indication of the effect of known systematic error in the results, it is pertinent to describe the setup used for the inferior measurements. First, the excitation light was filtered through 5 cm of aqueous $CuSO_4$ (200 g/l.) and a Corning 7-60 glass filter. This combination isolated the region between 330 and 390 nm that contains both $\pi\pi^*$ and CT bands of the molecules. Second, the output filter system consisted of one 3-68 and two 3-67 Corning glass filters. These were later shown to cut off slightly the high-energy edge of some of the emission bands. Third, the reference signal was generated with a GE 929 photodiode instead of the 9558QC photomultiplier. The GE 929 was subsequently shown to be slightly nonlinear in the uv region. Finally, the emission was viewed with a 9558QC photomultiplier whose quantum efficiency changes by almost 90% over the luminescence bandwidths of these complexes. In spite of the many uncertainties introduced by these less than optimum components, the relative quantum yields obtained by this experimental setup did not differ as much as expected from the other superior arrangement. The deviations of the two sets of measurements are portrayed in Figure 3 for $[Ru(bpy)_3]Cl_2$. Analogous data plots for the other molecules were similar. Computer analyses of the less precise data yielded radiative rate constants that differed slightly (<10%) from the better data; the major patterns and trends were not modified, however.

Results

Absorption and luminescence spectra of $[Ru(4,4'-Me_2bpy)_3]Cl_2$ in the alcohol medium are presented in Figure 4. We note that methyl substitution has modified the bands corresponding to those of the parent $[Ru(bpy)_3]Cl_2$ complex only slightly.[9] Neither the main charge-transfer absorption region maximizing at 458 nm nor the $\pi\pi^*$ absorption band peaking at 286 nm is shifted measurably by methyl substitution. The CT luminescence band has, however, been red shifted ~0.3 kK from its position in the parent

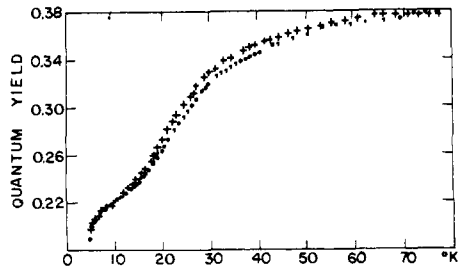

Figure 3. Quantum yield data for $[Ru(bpy)_3]Cl_2$ obtained under two sets of experimental parameters: ++++, EMI 9558QC photomultiplier, $CuSO_4$ + Corning 7-60 excitation filter, two Corning 3-67 + one Corning 3-68 emission filter; ····, RCA C31034 photomultiplier, $CuSO_4$ + Corning 7-59 + Optics Technology 450 redpass excitation filter, two Corning 3-69 emission filter.

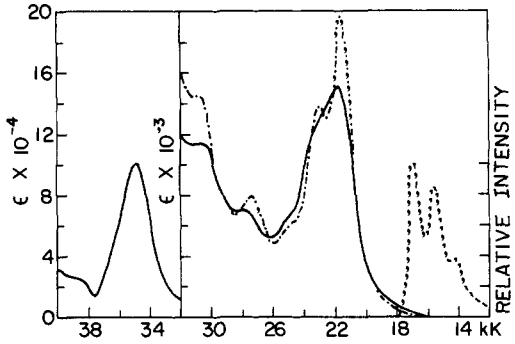

Figure 4. Absorption and luminescence spectra of $[Ru(4,4'\text{-}Me_2bpy)_3]Cl_2$ in ethanol–methanol (4:1, v/v): (—) absorption at room temperature; (- · -) absorption at 77 K (a 20% contraction of the glass has been assumed); (- - -) luminescence at 77 K.

molecule. The ~1.3-kK vibrational progression, indicative of a CT luminescence,[15] is clearly displayed.

Shown in Figure 5 are the luminescence spectra at 4.2 and 77 K of the three complexes doped in PMM matrices. The basic similarities among the spectra are obvious. All lie between 10 and 18 kK; all display the ~1.3-kK vibrational progression typical of these systems; none undergoes unusual sharpening as the temperature is varied. Significant spectral changes do occur, however, between 4.2 and 77 K. In all three cases the second prominent peak grows in at the expense of the highest energy adjacent peak as the temperature is lowered. Thus, the intensity distribution changes considerably, although the basic envelope structure remains.

As demonstrated in Figure 6 the lifetimes of all three complexes increase manyfold as the temperature is lowered from 77 to ~1.8 K, the changes being most pronounced below 10 K. At the same time the relative intensity of luminescence, and by inference the quantum yield, of each of the three complexes decreases monotonically as the temperature is lowered from 77 to 4.5 K.

To convert to absolute yields the relative intensity curves in the plastics were normalized to the known quantum yields measured in the ethanol–methanol glasses at 77 K. This procedure was adopted because an optically clear glass of the alcohol mixture could be maintained for quantum yield measurements at 77 K. To transfer the yields measured under these conditions to the species dissolved in PMM requires some justification. Measurements of the decay times of several of the complexes at 77 K were carried out both in the ethanol–methanol glass and in the PMM matrix. For all samples tested the values are slightly shorter in the PMM matrix compared with their values in the alcohol glass. The discrepancies range from 3 to 8% and are molecule dependent. We suspect that all of this change

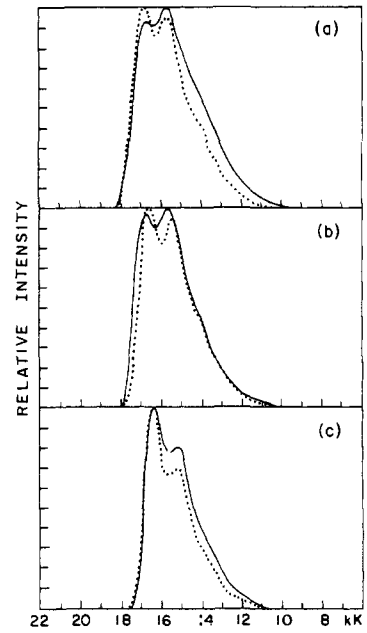

Figure 5. Luminescence spectra of ruthenium(II) complexes in PMM: (a) $[Ru(bpy)_3]Cl_2$, (b) $[Ru(4,4'\text{-}Me_2bpy)_3]Cl_2$, (c) $[Ru(4,4'\text{-}Ph_2bpy)_3]Cl_2$; (—) 4.2 K, (· · ·) 77 K.

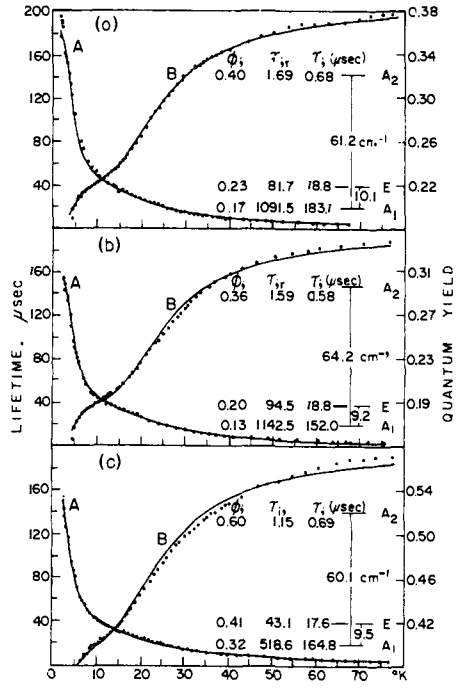

Figure 6. Temperature dependence of the lifetimes and quantum yields of ruthenium(II) complexes and computer generated parameters for each luminescing charge-transfer manifold: (a) $[Ru(bpy)_3]Cl_2$ in PMM, (b) $[Ru(4,4'\text{-}Me_2bpy)_3]Cl_2$ in PMM, (c) $[Ru(4,4'\text{-}Ph_2bpy)_3]Cl_2$ in PMM; (· · ·) experimental values, (—) "best fit" computer generated curves. Lifetimes, curve A, are read from the left ordinate; quantum yields, curve B, from the right.

can be attributed to an increase in the quenching constants and thus to a lower quantum yield in the plastic. Since the systematic error in the quantum yields measured in the alcohol glass could easily exceed 10%, however, we have chosen to adopt the values measured in the glass for the PMM matrix also. Thus, we attribute the large variations in decay times and quantum yields depicted in Figure 6 to molecular properties independent of the chosen matrix.

Phenomenological Model. To explain the steep increase of the measured lifetime and the concomitant decrease in

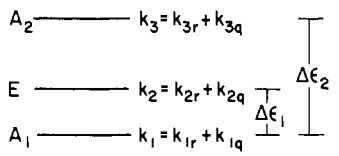

Figure 7. Schematic diagram of emitting charge-transfer states of trigonal ruthenium(II) complex ions: k_{ir}, radiative rate constant; k_{iq}, radiationless rate constant for conversion of the ith level to ground state. Proposed symmetry labels are for complexes of D_3 symmetry containing π-conjugated ligands.

the relative intensity of luminescence that occur as the temperature is lowered, a multiple state model of charge-transfer luminescence has been proposed.[4] The physical assumptions of the model are (a) the CT luminescence in these D_3 complexes is a superposition of the emissions of three closely spaced electronic states, (b) each of the sublevels is capable of coupling with the ground state either radiatively or radiationlessly, and these pathways are controlled by first-order kinetics with temperature independent rate constants, k_r and k_q, (c) Boltzmann equilibrium is established and maintained in time domains much shorter than the characteristic lifetimes of any of the sublevels, and (d) the manifold of luminescing states is populated from higher excited states with near unit efficiency at all temperatures and this efficiency is independent of excitation wavelength. The posited excited state description is depicted in Figure 7.

Based on the physical assumptions about the nature of the charge-transfer luminescing states stated above, analytical expressions giving both the lifetime and quantum yield of a complex as functions of temperature can be derived. (See appendix.) The temperature dependence of the lifetime of a manifold of decaying excited states in thermal equilibrium has been given by Azumi, O'Donnell, and McGlynn.[16] The expression, derived in the appendix, appropriate for the systems under discussion here is

$$\tau(T) = \frac{1 + 2e^{-\Delta\epsilon_1/kT} + e^{-\Delta\epsilon_2/kT}}{k_1 + 2k_2e^{-\Delta\epsilon_1/kT} + k_3e^{-\Delta\epsilon_2/kT}} \quad (1)$$

where the rate constants and energy gaps correspond to those defined in Figure 7.

Employing the same assumptions delineated above, one can derive an expression for the functional dependence of the quantum yield on temperature. The result, also derived in the appendix, is

$$\phi(T) = \frac{k_{ir} + 2k_{2r}e^{-\Delta\epsilon_1/kT} + k_{3r}e^{-\Delta\epsilon_2/kT}}{k_1 + 2k_2e^{-\Delta\epsilon_1/kT} + k_3e^{-\Delta\epsilon_2/kT}} \quad (2)$$

We note here that the second level of the manifold has been assigned a degeneracy of two. This factor appears both in the $\tau(T)$ and $\phi(T)$ expressions above. Although not derivable from the experimental data reported here, our proposed theoretical model requires a twofold degeneracy for the intermediate level (vide infra). We have therefore incorporated this factor in the data reduction procedures.

Figure 7 and eq 1 and 2 define the luminescing manifold completely. In principle a simultaneous computer fit of both $\tau(T)$ and $\phi(T)$ to the measured data points in Figure 6 should yield all the parameters defined. The actual data reduction procedure is detailed in a later section. The resultant level schemes are included in Figure 6. Extension to a three-level scheme is justified by the fact that an acceptable two-level fit could not be generated by the computer. Inclusion of a fourth level was unjustified since a three-level fit was manifestly adequate. Support for the assumed three-level scheme also comes from our theoretical model discussed below.

Group Theoretic Model for Charge-Transfer Luminescence. To rationalize the existence of three closely spaced electronic emitting states possessing the properties dictated by our analysis of the experimental data, we invoke the following simple group theoretic model of charge-transfer luminescence. First we imagine the optical electron as having been completely removed from the metal core, creating a d^5 complex in its ground state. The ground level of the resultant Ru(III) system is known to be a strongly spin-orbit coupled E′, where E′ is the spinor representation of the D_3* double group.[17] The optical electron with spin = E′ is now placed in the symmetric (with respect to the threefold axis) combination of the lowest unoccupied antibonding orbitals of the three ligands. This orbital transforms as a_2 in the group D_3.[18] The symmetries of the microstates resulting from this core-state coupling with the excited ligand electron are found by reducing the direct product, $(E')_{core} \times (E' \times a_2)_{ligand}$ in D_3*. They are A_1, A_2, and E. In the absence of coupling, these states are accidentally degenerate. Splitting occurs as the excited electron on the ligand is allowed to interact through coulombic forces with the spin-orbit coupled E′ core state. In this simple model the resultant splitting patterns (Figure 6) are interpreted as being due to weak exchange forces between the promoted electron and the d^5 core. Further implications of this model for the disposition and character of CT excited states are explored in the third paper of this series. Here we restrict attention to the *lowest* excited manifold that is manifested by the luminescence.

Data Reduction. The temperature dependent lifetime and quantum yield data for each complex were analyzed using a multiparameter least-squares curve-fitting computer program. Based on the Newton–Raphson method with internally approximated gradients,[19] this program was capable of analyzing data in terms of functional forms that contained up to 20 parameters in five independent variables. The lifetime data for a given complex were analyzed first. The derived expression contains five parameters, three total rate constants, and two energy gaps (eq 1). Numerical values for these quantities were determined by finding that unique set of parameters that generated the "best fit" of the equation to the data points generated by the flash measurements. Next, the corresponding quantum yield data of the complex were analyzed. A set of parameters was generated to provide a "best fit" of the quantum yield expression, $\phi(T)$, to the experimental data. In this second data reduction step the total rate constants and energy gaps appearing in $\phi(T)$ were not varied. Instead they were assigned the fixed numerical values determined from the lifetimes in the first data reduction step. Thus, numerical values of the three remaining radiative rate constants contained in eq 2 for each sublevel were determined by the second procedure. Once the values of the radiative and total rate constants for the sublevels were determined, the quantum yields and quenching rate constants for them were easily calculated.

Although the use of curve-fitting techniques to extract physical parameters from experimental data is open to criticism, we wish to emphasize that a high degree of self-consistency of the results was required. The same total rate constant and energy gap values that were derived from the decay time measurements were also required to generate acceptable computer fits of the quantum yield data. The precision of the values of the energy gaps and rate constants obtained in this way has been assessed elsewhere.[4] Until independent measurements of the quantities are performed, we have no definitive methods of judging their reliability.

Discussion

The important results of this study are summarized in Figure 6, where, in addition to the experimental data, the

final analytical expressions for $\tau(T)$ and $\phi(T)$ generated by the computer are plotted. On the same figures we have plotted the energy-level diagrams, relaxation times, and quantum yields for the individual levels supplied by the computer "best fit" to the data of the two experimental curves. The results for all the ions are very similar. Each complex has a lowest long-lived level followed by a second level $\sim$10 cm^{-1} away that decays somewhat less than ten times faster than the first one. A third level $\sim$60 cm^{-1} higher than the lowest one decays 25–30 times faster than the second. Previously we tentatively assigned the lowest level to A_1 (forbidden), the second to E (x,y-allowed), and the highest to A_2 (z-allowed) symmetry in D_3 on the basis of these measured lives only.[4] Our present data fully corroborate these assignments. In fact, we see that a comparison of *radiative* lives shows that the second level decays 12 times faster than the first and the third level decays 37–60 times faster than the second. Thus, radiative lives point again to a forbidden level lying lowest followed by two levels of varying degrees of allowedness. In previous work we labeled them A_1, E, and A_2, respectively, on the basis of a qualitative singlet-triplet argument that we no longer consider appropriate because of the strong spin-orbit coupling present in these systems. Nonetheless our previous assignments are verified quantitatively by the radiative decay rates extracted from the data. They are also justified theoretically by the coupling model presented in the third paper of this series. We have labeled the levels appropriately in the figure.

The individual quantum yields listed in Figure 6 also follow qualitative expectations. The electronically forbidden level has the smallest luminescence yield, and the quantum yields of the other two parallel their radiative decay rates. The uppermost level, which has the shortest radiative decay time, also displays the highest yield, a rational result.

The present analysis shows that the level scheme and assignments inferred previously[4] withstand the test of additional experimental evidence. The current data also indicate that the methods of measurement and data reduction employed can supply both radiative and radiationless decay parameters of the individual luminescing sublevels as well as the level splittings. Further discussion of these parameters, especially their relationship to the detailed molecular structures of the individual complexes, is contained in the second paper of this series where additional data on *o*-phenanthroline complexes are presented.

Once one accepts the existence of the excited state manifolds depicted for these systems, then several means of further testing the scheme and exploring its consequences unfold. First, any hope of resolving the band structures sufficiently to observe the origins of the separate transitions directly is dashed by the diffuseness of the spectra displayed in Figures 4 and 5. Individual peaks are $\sim$300 cm^{-1} wide even at 4.2 K, whereas the predicted levels are $<$100 cm^{-1} apart. Thus, unless some matrix capable of sharpening the spectra by an order of magnitude is found, direct observation of the separate band origins for the allowed transitions is precluded. Band shape changes do occur as the temperature is varied, but, in our opinion, they are more properly related to apparent shifts dictated by vibronic coupling mechanisms and changing Boltzmann factors associated with each of the electronic states and not to the simple resolution of separate transitions.

In the appendix we have derived expressions for the percentage of emitted radiation arising from each of the sublevels (eq A7) as a function of the energy gaps and decay parameters for the luminescing manifold. Substitution of the known values of these parameters obtained from the computer fits permits a computation of the fraction of radiation originating at each electronic level at any given temperature. These fractional intensities are plotted in Figure 8. The similarities of the level structures of these three systems are reflected in the fractional intensities. At 77 K, $\sim$90% of the photoluminescence from each of the species arises from the A_2 (z-allowed) electronic level. As the temperature decreases, this fraction steadily decreases as the Boltzmann factors change. Finally, at 10 K, the A_2 level is responsible for a negligible amount of the luminescence observed from each of the complexes. The E (x,y-allowed) level contributes about 10% of the emitted radiation at 77 K, a fraction that maximizes at a value greater than 75% at about 12 K. Below 10 K its contribution falls precipitously, becoming negligible below 2 K. The intensity of the radiation emanating from the A_1 (forbidden) level becomes significant only below 25 K, approaching 100% as $T \rightarrow 0$.

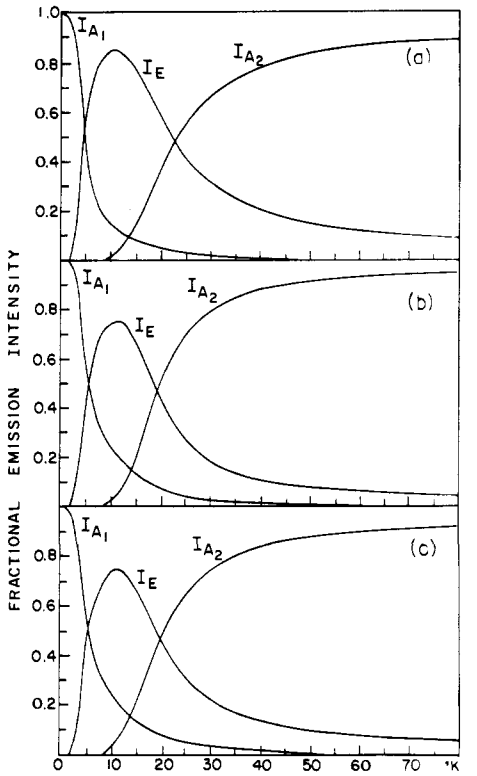

Figure 8. Temperature dependence of the fractional intensity of light emanating from the A_1, E, and A_2 states of (a) $[Ru(bpy)_3]Cl_2$, (b) $[Ru(4,4'\text{-}Me_2bpy)_3]Cl_2$, and (c) $[Ru(4,4'\text{-}Ph_2bpy)_3]Cl_2$ in PMM.

It is obvious from the figure that the electronic polarization should switch from essentially z to predominantly x,y as the temperature falls from 77 to $\sim$12 K. Thus, relative polarization measurements should be expected to supply confirmations for the electronic assignments. Aside from the experimental problems associated with obtaining reliable polarization measurements there are other factors peculiar to these complexes that may vitiate any conclusions drawn from such experiments. First, as shown in Figure 5 the vibrational bands are diffuse; there is little possibility of viewing the polarizations of the zero-phonon transitions of the two allowed bands, since the origins should be separated by only $\sim$50 cm^{-1}. One would be restricted to measuring the relative polarization of the whole band envelope or, at least, to monitoring one of the prominent peaks. Adjusting the temperature would, as discussed above, permit one to weigh one allowed state heavily, for instance, the E(x,y) state at $\sim$12 K. As shown in Figure 5, the spectra do not change very much as the temperature is varied. One concludes that the frequency distributions of the two allowed transitions must be quite similar. Thus, it is not likely that the polarization information buried under the band enve-

lope will provide definitive corroborative evidence for our proposed electronic state assignments.

The forbidden A_1 state is a special case. If the state is truly A_1, then all of the emitted light must be a consequence of some vibronic borrowing mechanism. Indeed, at very low temperatures (Figure 8) it should be possible to measure both the spectrum and the wavelength dependence of the polarization of the emission band, thus to obtain definitive vibronic coupling information. Measurements of the spectrum of $[Ru(bpy)_3]^{2+}$ in a crystalline host at ~1.6 K show that the first prominent peak at ~17 kK has virtually disappeared, and a new spectrum is beginning to grow in with its first prominent peak red shifted about 400 cm^{-1} from the spectrum shown in Figure 5a.[20] This behavior is expected for a vibronically allowed transition that is showing up because of the discrimination against the other two electronically allowed levels dictated by their small equilibrium populations at the low temperature.

We now turn to the central question of the ultimate validity of the phenomenological model. We reiterate that the entire treatment of the data is based on the maintenance of Boltzmann populations of the postulated levels at all times and at all temperatures. Above 2 K we have no experimental evidence to the contrary, either for this bipyridine series or for any of the other molecules we have studied. The faithful linearity of our logarithmic decays for all molecules was somewhat surprising, since it is well known that equilibration among components of spin multiplets does not obtain at temperatures below ~7 K.[21] Since, in our systems, such equilibration is evidently maintained down to ~1.6 K, we infer that the strong spin–orbit coupling present in these complexes of ruthenium ties the spin and orbital motions so tightly together that every state contains a high degree of orbital parentage. Thus the observed states are coupled to the molecular frame and hence are coupled strongly to the thermal motions of the solids. Equilibrium is maintained. In hydrocarbons the triplet states are virtually pure spin states due to the low atomic numbers and weak spin–orbit forces coupling the spins to the lattice motions. Thermal equilibrium is not maintained at low temperatures. The disparate thermal behaviors of these CT excited states of heavy metal complexes and the well-studied triplet states of aromatic molecules are indicative of the major role played by spin–orbit coupling in governing the dispositions and properties of CT levels. We explore this role mathematically in paper III of this series.

Our attention in this work has been directed toward ruthenium(II) complexes containing π-conjugated ligands. In particular we have limited our analysis to complexes of D_3 symmetry. We can report, however, that similar spectroscopic behavior has been observed for ruthenium(II) complexes containing terpyridine ligands (D_{2d} symmetry) and for five cis iridium(III) complexes containing bipyridine and *o*-phenanthroline as ligands that are of C_2 symmetry.[22] (The decay time characteristics of *cis*-dicyanobis(2,2′-bipyridine)- and *cis*-dicyanobis(1,10-phenanthroline)ruthenium(II) have already been reported.[4]) Iridium(III) complexes are expected, on theoretical grounds, to possess CT excited states analogous to the ones posited here for ruthenium(II) species. All these molecules and ions mentioned display CT luminescence, exponential decays, and strong temperature dependences of both the decay times and the quantum yields, similar to those reported here. Since the systems are of lower symmetry, no degeneracies are permitted and the coupling model loses some of its appealing simplicity. It is gratifying to find that three-level computer fits cannot be found for most of these other systems except over a restricted temperature range; we must go to four levels. Qualitatively, this behavior is expected since the central metal ion in a d^5 configuration is a Kramers ion and must possess a twofold degenerate ground state. Coupling this state with the promoted optical electron on the ligand system should give rise to four levels, just what the data require. Osmium(II) complexes are under investigation. They too display intense luminescences that are CT in nature[23] and strong thermal dependences of their decay times and intensities.[24] A model similar to that proposed here may apply, but the combined effects of the unusually large spin–orbit coupling inherent in the osmium atom and its low oxidation potential have not been fully explored. It appears, however, that the general model of CT luminescence proposed here is extensible, at least in principle, to other d^6 complexes of the second- and third-row transition elements that display low-lying CT excited states.

Other current investigations in this laboratory are supplying additional evidence that rapid relaxation among spin–orbit coupled excited states at sub-10 K temperatures is the rule and not peculiar to CT excited states. Our measurements of the temperature dependent lifetimes of both ruthenocene[25] and the hexacyanocobaltate ion[26] reveal exponential decays at all temperatures reached (<2 K), although the shapes of the resultant $\tau(T)$ curves are radically different from those reported here. Both these latter molecules display dd luminescence.

Appendix

To derive the expression for the decay time of an ensemble of excited systems in thermal equilibrium (eq 1), we assume a nondegenerate *p*-level manifold satisfying the criteria stated in the text (a-d, Phenomenological Model). At some time after the excitation flash, the rate of decay of the excited manifold is given by

$$dN/dt = \frac{d}{dt}\sum_{i=1}^{p} n_i = -\sum_{i}^{p} k_i n_i \qquad (A1)$$

where N = total population of the manifold at time t and k_i = total rate constant for depopulation of the ith level to the ground state. These k_i's do not include terms responsible for maintaining Boltzmann equilibrium among the individual levels.

Since the levels are assumed to remain in Boltzmann equilibrium during the decay process, we can write

$$n_i = Ne^{-\epsilon_i/kT} \Big/ \sum_{j=1}^{p} e^{-\epsilon_j/kT} \qquad (A2)$$

Substitution of eq A2 into A1 yields the expression

$$dN/dt = -\left(\sum_{i}^{p} k_i e^{-\epsilon_i/kT} \Big/ \sum_{j}^{p} e^{-\epsilon_j/kT}\right)N \qquad (A3)$$

Defining $\Delta\epsilon_{i-1} = \epsilon_i - \epsilon_1$ and multiplying both numerator and denominator of (A3) by $e^{\epsilon_1/kT}$, we obtain

$$dN/dt = -\frac{1}{\tau}N = -\left(\sum_{i}^{p} k_i e^{-\Delta\epsilon_{i-1}/kT} \Big/ \sum_{j}^{p} e^{-\Delta\epsilon_{j-1}/kT}\right)N \qquad (A4)$$

This is a first-order decay law with a decay time τ that is temperature dependent. By truncating the expression to conform to a three-level system possessing a twofold degenerate level, we produce eq 1 of the text.

The expression for the temperature dependence of the total quantum yield of an ensemble that is in Boltzmann equilibrium over a *p*-level manifold of nondegenerate levels proceeds as follows. We define ϕ, the total quantum yield of the ensemble, as the fraction of decaying systems that depopulate radiatively, i.e.,

$$\phi = \sum_{i=1}^{p} n_i k_{ir} \Big/ \sum_{j=1}^{p} n_j k_j \qquad (A5)$$

Since the system is under constant illumination and in thermal equilibrium, all the population numbers are time independent and are equal to the Boltzmann distribution numbers. Insertion of the expression for n_i from (A2) into (A5) and simplification produces the expression

$$\phi = \sum_{i=1}^{p} k_{ir} e^{-\epsilon_i/kT} \Big/ \sum_{j=1}^{p} k_j e^{-\epsilon_j/kT}$$

This equation is easily transformed into the final expression

$$\phi = \sum_{i=1}^{p} k_{ir} e^{-\Delta\epsilon_{i-1}/kT} \Big/ \sum_{j=1}^{p} k_j e^{-\Delta\epsilon_{j-1}/kT} \qquad \text{(A6)}$$

which becomes eq 2 in the text upon being particularized to a three-level manifold with a twofold degenerate second level.

We define I_i, the fraction of radiation originating at level i of the emitting manifold as the ratio of the rate of radiative decay from level i to the rate of radiative decay from all levels.

$$I_i = n_i k_{ir} \Big/ \sum_{i}^{p} n_i k_{ir}$$

Once again the insertion of Boltzmann distribution numbers and simplification of the result produces the desired expression

$$I_i = k_{ir} e^{-\Delta\epsilon_{i-1}/kT} \Big/ \sum_{j}^{p} k_j e^{-\Delta\epsilon_{j-1}/kT} \qquad \text{(A7)}$$

This equation, adapted to the appropriate level scheme, was used to generate the plots of Figure 8.

References and Notes

(1) Research supported by AFOSR(NC)-OAR, USAF Grant AFOSR-72-2207.
(2) Abstracted from a dissertation by G. D. Hager submitted to the Graduate School of Washington State University in partial fulfillment of the requirements for the degree Doctor of Philosophy, 1973.
(3) NDEA Fellow, 1968–1971.
(4) R. W. Harrigan and G. A. Crosby, *J. Chem. Phys.*, **59**, 3468 (1973); R. W. Harrigan, G. D. Hager, and G. A. Crosby, *Chem. Phys. Lett.*, **21**, 487 (1973).
(5) G. D. Hager, R. J. Watts, and G. A. Crosby, *J. Am. Chem. Soc.*, **97**, 7037 (1975).
(6) K. W. Hipps and G. A. Crosby, *J. Am. Chem. Soc.*, **97**, 7042 (1975).
(7) R. J. Watts and G. A. Crosby, *J. Am. Chem. Soc.*, **93**, 3184 (1971).
(8) D. H. W. Carstens and G. A. Crosby, *J. Mol. Spectrosc.*, **34**, 113 (1970).
(9) D. M. Klassen and G. A. Crosby, *J. Chem. Phys.*, **48**, 1853 (1968).
(10) J. N. Demas and G. A. Crosby, *J. Am. Chem. Soc.*, **93**, 2841 (1971).
(11) R. J. Watts and G. A. Crosby, *J. Am. Chem. Soc.*, **94**, 2606 (1972).
(12) R. J. Watts, unpublished results, this laboratory.
(13) R. W. Harrigan and G. A. Crosby, *Spectrochim. Acta, Part A*, **26**, 2225 (1970).
(14) "RCA Photomultiplier Tubes," Technical Publication PIT-700B, Radio Corp. of America, Dec 1971, pp 56–57.
(15) G. A. Crosby, R. J. Watts, and D. H. W. Carstens, *Science*, **170**, 1195 (1970).
(16) T. Azumi, C. M. O'Donnell, and S. P. McGlynn, *J. Chem. Phys.*, **45**, 2735 (1966).
(17) J. S. Griffith, "The Theory of Transition-Metal Ions", Cambridge University Press, Cambridge, England, 1971.
(18) L. E. Orgel, *J. Chem. Soc.*, 3683 (1961).
(19) M. J. D. Powell, *Comput. J.*, **7**, 303 (1965).
(20) D. C. Baker and G. A. Crosby, *Chem. Phys.*, **4**, 428 (1974).
(21) M. A. El-Sayed, *Acc. Chem. Res.*, **4**, 23 (1971).
(22) R. J. Watts and G. A. Crosby, unpublished results, this laboratory.
(23) B. J. Pankuch and G. A. Crosby, unpublished results, this laboratory.
(24) D. E. Lacky and G. A. Crosby, unpublished results, this laboratory.
(25) G. A. Crosby, G. D. Hager, K. W. Hipps, and M. L. Stone, *Chem. Phys. Lett.*, **28**, 497 (1974).
(26) K. W. Hipps and G. A. Crosby, *Inorg. Chem.*, **13**, 1543 (1974).

Charge-Transfer Excited States of Ruthenium(II) Complexes. II. Relationship of Level Parameters to Molecular Structure[1,2]

G. D. Hager,[3] R. J. Watts, and G. A. Crosby*

Contribution from the Department of Chemistry, Washington State University, Pullman, Washington 99163.

Received November 19, 1974

Abstract. Energy-level splittings and radiative and radiationless rate constants for the lowest excited $d\pi^*$ states of seven ruthenium(II) cations are compared and related to molecular structure. Exchange integrals between the promoted electron on the ligand system and the remaining core electrons have been calculated to lie in the range of 18–65 cm^{-1}, indicative of essential removal of the electron from the core during the excitation. Relationships between radiative and radiationless rate constants for individual levels have been demonstrated, and a dominant role for spin-orbit coupling in determining the energy-level splittings and promoting rapid relaxation among excited states has been assumed. Relations between excited state properties and chemical and electrochemical behavior are discussed.

Quantitative spectroscopic studies of the metal-to-ligand charge-transfer (CTTL) excited states of ruthenium(II) with bipyridine and substituted-bipyridine ligands have been reported in the preceding paper of this series.[4] The data strongly supported the previously proposed orbital and symmetry assignments of the lowest excited levels that are responsible for the observed photoluminescence.[5] In this article we present the results of extensive investigations of the properties of the lowest excited electronic states of ruthenium(II) complexes containing 1,10-phenanthroline and substituted 1,10-phenanthroline as ligands. The spectroscopic properties of these molecules not only corroborate the conclusions reached in the previous paper but, in conjunction with the other data, allow the detailed properties of the excited states of both series to be correlated with molecular structure.

Experimental Section

Synthesis and Sample Preparation. The tris(1,10-phenanthroline)ruthenium(II) iodide monohydrate, $[Ru(phen)_3]I_3$, was a sample prepared by Klassen.[6] Tris(4,7-diphenyl-1,10-phenanthroline)ruthenium(II) chloride pentahydrate, $[Ru(4,7\text{-}Ph_2phen)_3]Cl_2$, was prepared previously.[7] Both the tris(4,7-dimethyl-1,10-phenanthroline)ruthenium(II) chloride septahydrate, $[Ru(4,7\text{-}Me_2phen)_3]Cl_2$, and the tris(5,6-dimethyl-1,10-phenanthroline)ruthenium(II) chloride nonahydrate, $[Ru(5,6\text{-}Me_2phen)_3]Cl_2$, were prepared and purified by published methods for analogous compounds.[7]